

Calibrated Uncertainty Estimation Improves Bayesian Optimization

Shachi Deshpande¹, Volodymyr Kuleshov¹

¹Cornell University and Cornell Tech {ssd86, kuleshov}@cornell.edu

February 24, 2023

Abstract

Bayesian optimization is a sequential procedure for obtaining the global optimum of black-box functions without knowing *a priori* their true form. Good uncertainty estimates over the shape of the objective function are essential in guiding the optimization process. However, these estimates can be inaccurate if the true objective function violates assumptions made by its model (e.g., Gaussianity). This paper studies which uncertainties are needed in Bayesian optimization models and argues that ideal uncertainties should be calibrated—i.e., an 80% predictive interval should contain the true outcome 80% of the time. We propose a simple algorithm for enforcing this property and show that it enables Bayesian optimization to arrive at the global optimum in fewer steps. We provide a theoretical analysis that justifies the use of calibration and we demonstrate the improved performance of our method on standard benchmark functions and hyperparameter optimization tasks.

1 INTRODUCTION

Bayesian optimization has emerged as a powerful tool for tuning the hyperparameters of machine learning models [Shahriari et al., 2016, Thornton et al., 2013, Bergstra et al., 2011, Snoek et al., 2012]. In its general form, Bayesian optimization optimizes a black box objective function—i.e., a function that is initially unknown and that can be learned via a sequence of evaluation queries—by forming a probabilistic model that encodes beliefs about the shape of the function and by iteratively selecting query points according to this model. Crucially, this process needs to strike a balance between learning the unknown shape of the function and finding its minimum.

In practice, querying the black-box objective during optimization can be expensive: for example evaluating the objective function during hyperparameter optimization may involve training a machine learning model from scratch. Bayesian optimization aims to minimize the number of objective function queries by relying on its probabilistic model to guide search [Frazier, 2018]. Such probabilistic models are not always accurate and may be overconfident, which slows down optimization and may yield suboptimal local optima [Guo et al., 2017, Kuleshov et al., 2018].

This paper aims to improve the performance of algorithms for online sequential decision-making under uncertainty, particularly Bayesian optimization. We start by examining which uncertainties are needed in model-based decision-making and provide a theoretical analysis that argues that ideal uncertainties should be calibrated. Intuitively, calibration means that an 80% confidence interval should contain the true outcome 80% of the time. Calibrated predictive uncertainties help balance exploration and exploitation, estimate the expected value of the objective function, and reach the optimum in fewer steps.

Next, we introduce simple algorithms for enforcing accurate and calibrated uncertainties within the framework of Bayesian optimization. Our methods can be added to any Bayesian optimization algorithm with minimal modifications and with minimal computational and implementation overhead. Empirically, we show that our techniques yield faster convergence to higher quality optima across a range of standard benchmark functions and hyperparameter optimization tasks.

Contributions: In summary, this work makes the following contributions: (1) we provide a theoretical analysis of the uncertainties needed in online sequential decision making and argue that they need to be calibrated; (2) we introduce simple algorithms for enforcing calibrated uncertainties within any existing Bayesian optimization algorithm with minimal computational and implementation overhead; (3) we demonstrate that our methods accelerate search in hyperparameter optimization tasks.

2 BACKGROUND

2.1 Bayesian Optimization

Notation. Bayesian optimization is a technique for finding the global minimum $x^* = \arg \min_{x \in \mathcal{X}} f(x)$ of an unknown black-box objective function $f : \mathcal{X} \rightarrow \mathbb{R}$ over an input space $\mathcal{X} \subseteq \mathbb{R}^D$. We assume there exists a data distribution P over the features and labels $X, Y \in \mathcal{X} \times \mathbb{R}$, and we are given an initial labeled dataset $x_t, y_t \in \mathcal{X} \times \mathbb{R}$ for $t = 1, 2, \dots, N$ of i.i.d. realizations of random variables $X, Y \sim P$.

Computing $f(x)$ is usually computationally expensive; furthermore we may not have access to the values of f or its gradient. A classical application area of Bayesian optimization is hyperparameter search, where $x \in \mathcal{X}$ are choices of hyperparameters, and $f(x)$ is the resulting performance of a machine learning model.

Algorithm. We optimize f iteratively. At each step, we form a probabilistic model $\mathcal{M} : \mathcal{X} \rightarrow (\mathbb{R} \rightarrow [0, 1])$ of f . We use uncertainty estimates from this probabilistic model to pick an x_{next} and update \mathcal{M} iteratively. Algorithm 1 describes the basic Bayesian optimization loop.

Algorithm 1: Bayesian Optimization

```

Initialize base model  $\mathcal{M}$  with data  $\mathcal{D} = \{x_t, y_t\}_{t=0}^N$ ;
for  $n = 1, 2, \dots, T$  do
   $x_{\text{next}} = \arg \max_{x \in \mathcal{X}} \text{Acquisition}(x, \mathcal{M})$ ;
   $y_{\text{next}} = f(x_{\text{next}})$ ;
   $\mathcal{D} = \mathcal{D} \cup \{(x_{\text{next}}, y_{\text{next}})\}$ ;
  Update model  $\mathcal{M}$  with data  $\mathcal{D}$ ;
end

```

Acquisition Functions. Let x' be a prospective next point. The probability of improvement (PI) is an acquisition function specified by $\text{Acq}_{\text{PI}}(x, \mathcal{M}) = \arg \max_x (P(f(x) \geq (f(x') + \epsilon)))$. Similarly, the expected improvement (EI) can be written as $\text{Acq}_{\text{EI}}(x, \mathcal{M}) = \arg \max_x (E_f(\max(0, f(x) - f(x'))))$. Finally, the upper confidence bound (UCB) acquisition function is given by $\text{Acq}_{\text{UCB}}(x, \mathcal{M}) = Q_\gamma(x)$ where $Q_\gamma(x)$ is the conditional γ -th quantile of the distribution $\mathcal{M}(x)$.

2.2 Calibrated & Conformal Prediction

A classical approach in statistics for evaluating uncertainties are proper scoring rules [Gneiting and Raftery, 2007]. Proper scoring rules measure precisely two characteristics of a forecast: calibration and sharpness. Intuitively, calibration means that a 90% confidence interval contains the outcome about 90% of the time. Sharpness means that confidence intervals should be tight. Maximally tight and calibrated confidence intervals are Bayes optimal.

Calibration. Formally, suppose we have a model $H : \mathcal{X} \rightarrow (\mathbb{R} \rightarrow [0, 1])$ that outputs a probabilistic forecast F_x given an input x . We take F_x to be a cumulative distribution function (CDF) and we use $F_X^{-1}(p) = \inf\{y : F_X(y) = p\}$ to denote its inverse; we denote the density by f_x .

We say that H is **distribution calibrated** if the true density of Y conditioned on H matches its predicted density f : $P(Y | H(X) = f) = f \forall f$. A weaker notion is **quantile calibration**, defined as $P(Y \leq F_X^{-1}(p)) = p \forall p \in [0, 1]$. In an online setting this definition becomes

$$\frac{\sum_{t=1}^T \mathbb{I}\{y_t \leq F_t^{-1}(p)\}}{T} \rightarrow p \text{ for all } p \in [0, 1] \quad (1)$$

as $T \rightarrow \infty$, hence the predicted and empirical confidence intervals match.

Calibrated Prediction Out of the box, most models H are not calibrated. Calibrated and conformal prediction yield calibrated forecasts by comparing observed and predicted frequencies on a hold-out dataset [Shafer and Vovk, 2007, Kuleshov et al., 2018, ?, Vovk et al., 2020].

3 CHARACTERIZING UNCERTAINTY IN ONLINE DECISION-MAKING

3.1 Which Uncertainties Are Needed in Online Decision-Making?

When a predictive model is Bayes optimal, its forecasts are calibrated and sharp. However, most models are not optimal, and we need to balance these two distinct properties. This raises the question: are they equally important for downstream tasks such as online decision-making?

This paper demonstrates that the calibration-sharpness tradeoff significantly impacts downstream performance. In particular, we argue that it is much **better to be calibrated than sharp**. We provide intuitive and formal arguments for this claim, and then derive calibration algorithms that improve decision-making performance.

Why is Calibration Useful? A key challenge faced by decision-making algorithms is balancing exploration — e.g., the process of learning the shape of the unknown function f in Bayesian optimization — against exploitation—e.g., the process of selecting points x at which f takes small values. Exploration-exploitation decisions are often made using a probabilistic model. In regions that are unexplored, the confidence interval around the value of $f(x)$ should be large to promote exploration. Calibration helps mitigate over-confidence and promotes accurate confidence intervals that encourage exploration.

Another benefit of calibrated models is the accurate computation of expected values of future outcomes. Since an expectation is a sum weighted by probabilities of future events, aligning predicted and empirical probabilities is crucial. Accurate estimates of expected utility yield improved planning performance in model-based algorithms [Malik et al., 2019].

3.2 Theoretical Analysis

Next, we complement this intuition with a formal characterization of the benefits of calibration. We are interested in decision-making settings where we sequentially minimize a loss function $\ell : \mathcal{Y} \times \mathcal{A} \times \mathcal{X} \rightarrow \mathbb{R}$ over a set of outcomes \mathcal{Y} , actions \mathcal{A} , and features \mathcal{X} . The loss $\ell(y, a, x)$ quantifies the error of an action $a \in \mathcal{A}$ in a state $x \in \mathcal{X}$ given outcome $y \in \mathcal{Y}$.

Bayesian decision-making theory provides a principled approach for selecting actions in the above scenario. We rely on a predictive model H of y and select decisions that minimize the expected loss:

$$a(x) = \arg \min_a \mathbb{E}_{y \sim H(x)} [\ell(y, a, x)] \quad (2)$$

$$\ell(x) = \min_a \mathbb{E}_{y \sim H(x)} [\ell(y, a, x)]. \quad (3)$$

Here, $a(x)$ is the action that minimizes the expected loss under H . We study losses $\ell(y, a, x)$ that are monotonically non-increasing or non-decreasing in y . Examples include linear utilities $v(a, x) \cdot y + c(a, x)$ or their monotone transformations. Note that common acquisition functions used in Bayesian optimization fall in this framework.

Expectations Under Distribution Calibrated Models If H was a perfect predictive model, the above decision-making approach would be optimal. In practice, inaccurate models can yield imperfect decisions. Surprisingly, our analysis shows that in many cases, calibration (a much weaker condition than having a perfectly specified model H) is sufficient to correctly estimate the value of the loss function.

Theorem 1. *Let $Q(Y|X)$ be a distribution calibrated model over $X, Y \sim P$. Then, for any function $g : \mathbb{Y} \rightarrow \mathbb{R}$,*

$$\mathbb{E}_{y \sim P(Y)} [g(y)] = \mathbb{E}_{\substack{x \sim P(X) \\ y \sim Q(Y|X=x)}} [g(y)]. \quad (4)$$

Malik et al. [2019] proved this in discrete settings; we extend their result to general continuous variables (Appendix F).

Expectations Under Quantile-Calibrated Models. Surprisingly, the guarantees for distribution calibrated models can be obtained with a much weaker condition—quantile calibration. Additional requirements are the non-negativity and monotonicity of the loss. We start with a lemma.

Lemma 1. *Let $Q(Y|X)$ be a quantile calibrated model over $X, Y \sim \mathbb{P}$, $Y \geq 0$. Then the expectation of Y is the same under P and Q : $\mathbb{E}_{y \sim \mathbb{P}(Y)} [y] = \mathbb{E}_{x \sim \mathbb{P}(X)} \mathbb{E}_{y \sim Q(Y|X=x)} [y]$.*

We provide the proof in the Appendix F. We can use the above result to establish an analogue of the guarantee available for distribution calibration

Theorem 2. *Let $Q(Y|X)$ be a quantile calibrated model over $X, Y \sim P$. Then, for any non-negative monotonic function $g : \mathbb{Y} \rightarrow \mathbb{S}$ we have:*

$$\mathbb{E}_{y \sim P(Y)} [g(y)] = \mathbb{E}_{\substack{x \sim P(X) \\ y \sim Q(Y|X=x)}} [g(y)]. \quad (5)$$

This result follows from the previous lemma (see Appendix F). Since Q is a quantile calibrated model for Y , $g \circ Q$ is a quantile calibrated model for the random variable $g(Y)$ when g is monotonic: $P(g(Y) \leq g(Q_X(p))) = p$.

We further complement these results with concentration inequalities that show that estimates of the calibrated loss are unlikely to exceed the true loss. [Zhao et al., 2020]

Theorem 3. Let $Q(Y|X)$ be a quantile calibrated model and let $\ell(y, a)$ be a monotonic loss. Then we have for $t > 1$:

$$P(\ell(y, a(x)) \geq t\ell(x)) \leq 1/t \quad (6)$$

Note that this statement represents an extension of Markov inequality. We can also show that the same guarantees hold for distribution calibration, which is a stronger condition.

Corollary 1. Let $Q(Y|X)$ be a distribution calibrated model and let $\ell(y, a)$ be a monotonic loss. For $t > 1$:

$$P(\ell(y, a(x)) \geq t\ell(x)) \leq 1/t \quad (7)$$

These results provide theoretical justification about the value of calibration in decision-making. Next, we provide methods for approximately enforcing these in Bayesian optimization.

4 Calibrated Bayesian Optimization

We aim to improve the decisions made at every step in Bayesian optimization by calibrating the underlying model $\mathcal{M} : \mathcal{X} \rightarrow (\mathcal{Y} \rightarrow [0, 1])$. Algorithm 2 outlines our proposed procedure.

Algorithm 2: Calibrated Bayesian Optimization

```

Initialize base model  $\mathcal{M}$  with data  $\mathcal{D} = \{x_t, y_t\}_{t=0}^M$ ;
 $\mathcal{R} \leftarrow \text{CALIBRATE}(\mathcal{M}, \mathcal{D})$ ;
for  $n = 1, 2, \dots, T$  do
   $x_{\text{next}} = \arg \max_{x \in \mathcal{X}} (\text{Acquisition}(x, \mathcal{R} \circ \mathcal{M}))$ ;
   $y_{\text{next}} = f(x_{\text{next}})$ ;
   $\mathcal{D} = \mathcal{D} \cup \{(x_{\text{next}}, y_{\text{next}})\}$ ;
  Update model  $\mathcal{M}$  with data  $\mathcal{D}$ ;
   $\mathcal{R} \leftarrow \text{CALIBRATE}(\mathcal{M}, \mathcal{D})$ ;
end

```

Algorithm 2 mirrors standard Bayesian optimization, except that we compose \mathcal{M} with a recalibrator \mathcal{R} that takes a forecast F from \mathcal{M} and transforms it into a calibrated $\mathcal{R} \circ F$. By a slight abuse of notation, we denote this by $F = \mathcal{R}(\mathcal{M}(x))$. We treat \mathcal{M} as a black box.

Recalibrating a Bayesian Optimization Model. In Bayesian optimization, the dataset \mathcal{D} is usually small, and it is expensive to acquire more datapoints by evaluating f . To address this challenge, we develop a recalibration procedure that deals with small dataset sizes.

Algorithm 3 builds a recalibration dataset $\mathcal{D}_{\text{recal}}$ via cross-validation on \mathcal{D} . It leverages the recalibration algorithm based on Kuleshov et al. [2018] (Algorithm 4), which can be referred in Appendix B. At each step of cross-validation, we train a base model \mathcal{M}' on the training folds and compute forecasts on the test folds. The union of all the forecasts on the test folds produces the final calibration dataset on which the recalibrator is trained.

In our experiments, we used leave-one-out cross-validation within `CREATESPLITS`. Formally, given a dataset $\mathcal{D} = \{x_t, y_t\}_{t=1}^N$, `CREATESPLITS`(\mathcal{D}) produces N train-test splits of the form $\{(\mathcal{D} \setminus \{x_i, y_i\}, \{x_i, y_i\}) \mid i = 1, 2, \dots, N\}$. Thus, the base model \mathcal{M}' is trained on $(N-1)$ data-points in the train split and used to generate predicted output CDF for the only data-point $\{x_i, y_i\}, 1 \leq i \leq N$ within the test split. This process is repeated for each split, so that we have the output CDF for

Algorithm 3: CALIBRATE

Input: Base model \mathcal{M} , Dataset $\mathcal{D} = \{x_t, y_t\}_{t=0}^N$

1. Initialize recalibration dataset $\mathcal{D}_{\text{recal}} = \emptyset$
2. $S = \text{CREATE SPLITS}(\mathcal{D})$
3. For each $(\mathcal{D}_{\text{train}}, \mathcal{D}_{\text{test}})$ in S :
 - (a) Train base model \mathcal{M}' on dataset $\mathcal{D}_{\text{train}}$
 - (b) Create calibration set \mathcal{C} from $\mathcal{D}_{\text{test}}$
 - (c) $\mathcal{D}_{\text{recal}} = \mathcal{D}_{\text{recal}} \cup \mathcal{C}$
4. Train recalibrator model \mathcal{R} on the recalibration dataset $\mathcal{D}_{\text{recal}}$ using Algorithm 4
5. Return (\mathcal{R})

each of the N data-points from our original training dataset. The time complexity of Algorithm 3 depends linearly on the number of splits. The choice of model \mathcal{M} also influences the run-time of this algorithm. Please refer to Appendix D for further discussion.

4.1 Examining Acquisition Functions

The **probability of improvement** can be written as $1 - F_x(f(x^+) + \epsilon)$, where F_x is the CDF at x that is predicted by the model. In a quantile-calibrated model, this corresponds to the empirical probability of seeing an improvement and yields better decisions. The **expected improvement** can be defined as $\mathbb{E}[\max(f(x) - f(x^+), 0)]$. If we have a calibrated distribution over Y , it is easy to derive from it a calibrated distribution over the above reward; by Proposition 2 (Appendix F), we can provably estimate its expectation. **Upper confidence bounds** are $\mu(x) + \gamma \cdot \sigma(x)$ for Gaussians and $F_x^{-1}(\alpha)$ for general F . Recalibration adjusts confidence intervals such that $\alpha \in [0, 1]$ yields an interval that is above the true y a fraction α of the time. Appendix C discusses acquisition functions further.

5 EXPERIMENTS

We perform experiments on several benchmark objective functions that are standard in the Bayesian optimization literature, as well as on a number of hyperparameter optimization tasks.

Setup. We use the Gaussian Process (GP) as our base model in the following experiments. However, our method can be applied to any probabilistic model underlying Bayesian optimization in general [Snoek et al., 2015], [Springenberg et al., 2016]. In our implementation, we calibrate by mapping the standard deviation predicted by base model σ to σ_{new} such that the new CDF is calibrated according to the recalibration algorithm by Kuleshov et al. [2018] (Appendix B). Specifically, the standard deviation is increased or decreased to make sure that the uncertainty estimates derived from the resulting distribution are better calibrated. Leave-one-out cross-validation splits and time-series splits are used in the `CREATE SPLITS` function in Algorithm 3. We use another GP as our recalibrator model \mathcal{R} . Further details on the implementation can be found in the Appendix A.

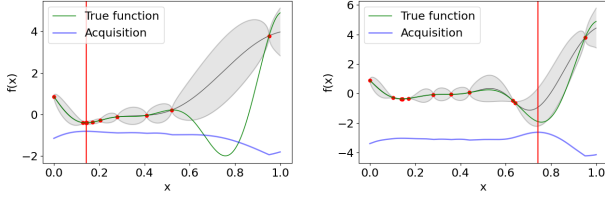


Figure 1: Comparison of Uncalibrated and Calibrated Bayesian Optimization on the Forrester Function (green) Using the UCB Acquisition Function (blue).

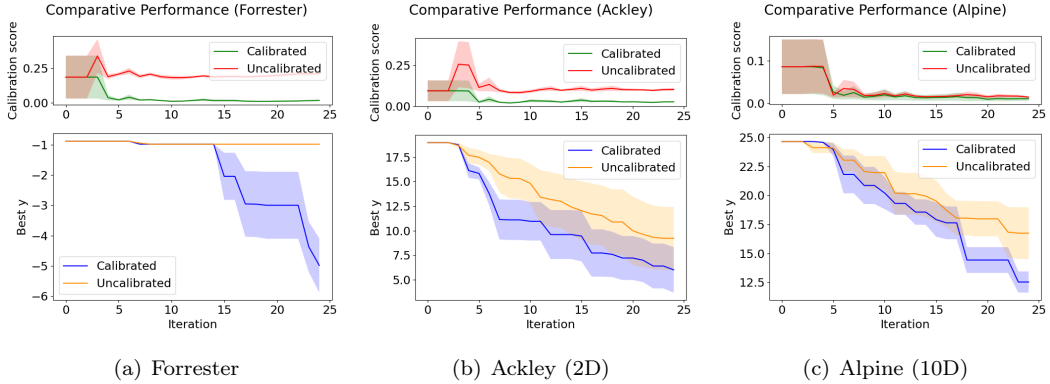


Figure 2: Comparison of Bayesian optimization in Benchmark Functions. In the top plots, we see that calibrated method produces lower average calibration scores at every step. The bottom plots show that on an average, the calibrated method (blue) dominates the uncalibrated method (orange) by achieving the minimum value of function using less number of steps.

Analysis of Calibration. We assess the calibration of the original probabilistic model underlying Bayesian optimization using calibration scores as defined by Kuleshov et al. [2018]. Thus, $\text{cal}(F_1, y_1, \dots, F_n, y_n) = \sum_{j=1}^m (p_j - \hat{p}_j)^2$, where $0 \leq p_1 < p_2 < \dots < p_m \leq 1$ are m confidence levels using which we compute the calibration score. \hat{p}_j is estimated as $\hat{p}_j = |\{y_t | F_t \leq p_j, t = 1, \dots, N\}|/N$. The calibration scores are computed on a test dataset $\{F_t, y_t\}_{t=0}^T$. This test dataset is constructed by setting $F_t = F_{x_{\text{next}}}(y_{\text{next}})$ and $y_t = y_{\text{next}}$ at every step t before updating model \mathcal{M} in Algorithm 2. In our experiments, we average the calibration score at every step of Bayesian optimization over 5 repetitions of the experiment for each benchmark function.

5.1 Benchmark Optimization Tasks

We visualize runs of calibrated and plain Bayesian optimization on a simple 1D task — the Forrester function in Figure 1. We use the Upper Confidence Bound (UCB) as our acquisition function. Both functions start at the same three points, which miss the global optimum in $[0.6, 0.9]$. The base GP is overconfident, and never explores that region. However, the calibrated method learns that its confidence intervals are uncalibrated and too narrow; thus, it expands them. This leads it to immediately explore in $[0.6, 0.9]$ and find the global optimum. The uncalibrated method gets forever stuck at a local minimum near 0.2. We observed similar behavior on many repetitions of

this experiment. On some repetitions, the initial points were sampled sufficiently close to the global optimum, and the two methods performed similarly. Nonetheless, this experiment provides a concrete example for why calibration can improve Bayesian optimization. Please refer to Appendix E for additional plots.

In Figure 2(a), we can see that the calibrated method was able to search the global minimum before the uncalibrated method for the Forrester function. In Figure 2(b) and Figure 2(c), we compare the performance of calibrated method against uncalibrated method under EI acquisition function on the 2D Ackley function and 10D Alpine function [Surjanovic and Bingham]. In Figure 3, we compare the performance of our method on the Sixhump Camel function while varying the acquisition function. In all these examples, we see that the calibrated method finds the minimum before the uncalibrated method on an average.

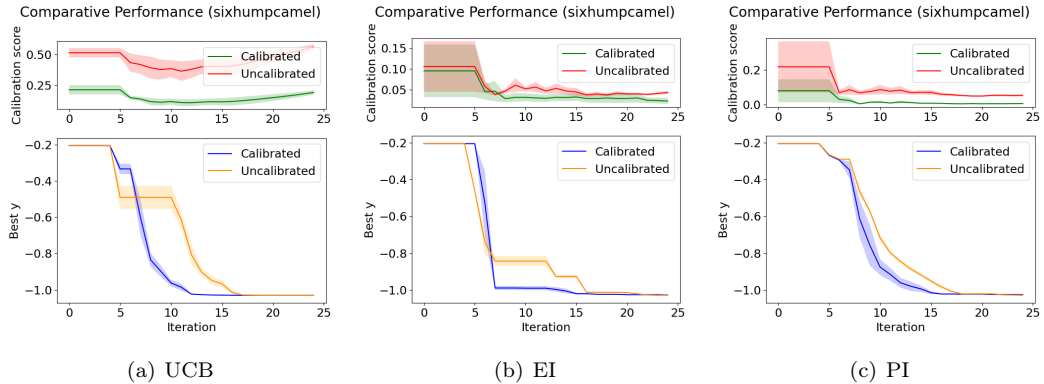


Figure 3: Comparison of Bayesian Optimization in Six-hump-camel Function (2D). We compare the effect of calibration under different acquisition functions. The top plots show that average calibration error at every step is lower with the calibrated method. In the bottom plots, we see that on an average, the calibrated method (blue) dominates the uncalibrated method (orange) by achieving the minimum value of function using less number of steps in Bayesian optimization.

Comparison Against Additional Baselines. In Table 1, we compare our method against baselines including input and output warping [Snoek et al., 2014, Snelson et al., 2004], Box-Cox and log-transforms on the output [Rios and Tobar, 2018] and a method to improve uncertainty estimation (an ensemble of Gaussian processes [Lakshminarayanan et al., 2016]). Metrics used to perform this evaluation include the minimum value m of the objective function achieved by Bayesian optimization, fraction f of experimental repetitions where the baseline performs worse than our method and normalized area under the Bayesian optimization curve a . Please refer to Appendix A.1 for detailed definition of these metrics.

In Table 1, we see that warping methods occasionally improve over the uncalibrated method, often worsen it, and recalibration is almost always more effective than warping. Both uncertainty estimation methods (ensembling and calibration) improve performance relative to the uncalibrated method, with calibration yielding the bigger improvement.

Additional Optimization Tasks. In Table 2, we evaluate our method on seven additional optimization tasks [Surjanovic and Bingham], consisting of objective functions that are often used in the Bayesian optimization literature to evaluate optimization algorithms. We fixed the choice of

Table 1: Comparison of Calibrated Bayesian Optimization Against Baselines. We see that the calibrated method compares favorably against Input warping [Snoek et al., 2014], Output warping (tanh as in [Snelson et al., 2004]), Boxcox and Log transformation of output [Rios and Tobar, 2018], and Bagged ensemble of 5 GPs [Lakshminarayanan et al., 2016].

Objective Function	Method	Minimum Found (\downarrow)	Fraction of Runs Where Calibrated Beats Baseline (\uparrow)	Area Under the Curve (\downarrow)
Forrester (1D)	Calibrated Method	-4.983 (0.894)	1	0.8187
	Uncalibrated method	-0.986 (0.001)	0.8	0.9866
	Input warping	-0.889 (0.000)	1	1.0000
	Output warping	-6.021 (0.000)	0.0	0.2409
	Boxcox transformation of output	-4.806 (0.780)	0.4	0.4911
	Log transformation of output	-0.986 (0.000)	1	0.9865
	Bagged ensemble of 5 GPs	-3.891(1.098)	0.8	0.8382
Ackley (2D)	Calibrated Method	5.998 (2.314)	1	0.5516
	Uncalibrated method	12.359 (2.439)	0.8	0.7815
	Input warping	14.061 (1.312)	0.8	0.8125
	Output warping	10.459 (3.365)	0.6	0.7257
	Boxcox transformation of output	14.421 (1.423)	0.8	0.9015
	Log transformation of output	8.330 (0.849)	0.8	0.6524
	Bagged ensemble of 5 GPs	6.011 (2.544)	0.6	0.6013
Alpine (10D)	Calibrated Method	12.537 (0.909)	1	0.6423
	Uncalibrated method	15.506 (1.275)	0.6	0.6527
	Input warping	15.697 (1.740)	0.8	0.6492
	Output warping	13.531 (2.127)	0.6	0.5857
	Boxcox transformation of output	15.715 (0.603)	0.8	0.6253
	Log transformation of output	20.996 (1.661)	0.8	0.7931
	Bagged ensemble of 5 GPs	16.677 (1.699)	0.8	0.7334

Table 2: Evaluating Calibrated Bayesian Optimization on Additional Tasks. Calibration strictly improves performance on four benchmark tasks while the performance is similar on two tasks. The performance degradation in Cross-in-Tray function could be attributed to the presence of multiple sharp edges and corners that are hard to model through GP.

Optimization benchmark	% Runs Where Calibrated is Best (\uparrow)	Area Under the Curve, Calibrated (\downarrow)	Area Under the Curve, Uncalibrated (\downarrow)
Cosines	0.8	0.2973	0.3395
Beale	0.6	0.0929	0.0930
Mccormick	0.8	0.1335	0.1297
Powers	0.8	0.2083	0.2325
Cross-in-Tray	0.2	0.2494	0.2217
Ackley	0.8	0.3617	0.4314
Dropwave	0.6	0.0455	0.0452

hyperparameters in the calibration algorithm (3 randomly chosen initialization points, Matern kernel, PI acquisition, time-series splits and 25 BO steps).

The Dropwave and Beale functions are examples of where both methods perform the same. We believe that since the Cross-in-Tray function has multiple sharp edges, it is significantly harder for the GP to model it, and our method may need some improvements to work well with these kinds of functions. On the McCormick function, the uncalibrated method makes more progress in the initial stages, but the calibrated method finds the minimum earlier.

Sensitivity Analysis. We perform a sensitivity analysis of our method over its hyper-parameters

Table 3: Sensitivity Analysis of Calibrated Bayesian Optimization (Algorithm 2 and 3) for the Forrester Function.

Hyper-Parameter	Modification	% Runs Where Calibrated is Best (\uparrow)	Area Under the Curve, Calibrated (\downarrow)	Area Under the Curve, Uncalibrated (\downarrow)
Kernel of Base Model \mathcal{M}	Matern	0.8	0.2811	0.3454
	Linear	1.0	0.5221	1.0000
	RBF	0.4	0.2366	0.2922
	Periodic	0.6	0.2586	0.3305
Recalibrator Model \mathcal{R}	GP	0.8	0.2810	0.3454
	MLP	0.8	0.2785	0.3454
Number of Data Points for Initializing Base Model	3	0.8	0.2810	0.3454
	4	0.8	0.0557	0.0614
	7	0.4	0.0719	0.0736
	10	0.4	0.0825	0.0817
Acquisition function (Linear kernel)	LCB	1.0	1.0000	1.0000
	EI	1.0	0.5221	1.0000
	PI	0.8	0.6920	1.0000

for the Forrester function. Our results in Table 3 indicate that calibration provides performance improvements across a range of settings, specifically over different kernel types, acquisition functions, and recalibration strategies. Appendix A.3 contains additional results on sensitivity analysis.

5.2 Hyperparameter Optimization Tasks

5.2.1 Online LDA

In the Online LDA algorithm [Hoffman et al., 2010], we have three hyperparameters: τ_0 and κ which control the learning rate and minibatch size s (Appendix A.4). The objective function takes these hyperparameters as input and runs the Online LDA algorithm to convergence on the training set. It outputs perplexity on the test dataset. We run this experiment on the 20 Newsgroups dataset. In Figure 4(a), we see that the calibrated method achieves a configuration of hyperparameters giving lower perplexity on an average. We see that the error bars around the averaged runs are intersecting significantly as there was more variation across experiment repetitions. Hence, we add a separate plot showing the average of improvement made by the calibrated method over uncalibrated method during individual runs of the experiment. Formally, the improvement at any given iteration of Bayesian optimization is the difference between the best minimum found by uncalibrated method and the best minimum found by calibrated method. We see that the average improvement made by the calibrated method and the error bars surrounding it are positive most of the time.

5.2.2 Image Classification Using Neural Networks

We define a Convolutional Neural Network (CNN) for image classification with 6 tunable hyperparameters – batch-size, learning-rate, learning-rate decay, l2-regularization, number of convolutional filters and number of neurons in the fully connected layer (Appendix A.5). With these hyperparameter values as input, our objective function trains the CNN and returns the classification error on test dataset. We use Bayesian optimization to search for an optimum configuration of hyperparameters that results in lower classification error. We run our experiments on CIFAR10 [Krizhevsky, 2009] and SVHN datasets [Netzer et al., 2011]. On the CIFAR10 dataset (Figure 4(b)), we see that the calibrated method achieves a lower classification error on an average at the end of 50 iterations of Bayesian

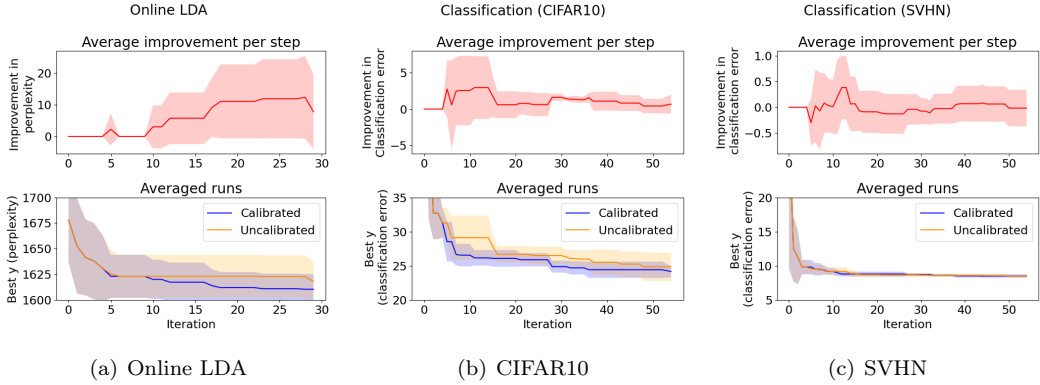


Figure 4: Comparison of Bayesian optimization in Hyperparameter Optimization tasks. The top plots in red show the average of improvement made by the calibrated method over uncalibrated method during individual runs of the respective experiment. In the plots on the bottom, the blue and orange lines correspond to average of the best minimum found by Bayesian optimization at a given iteration, for calibrated and uncalibrated method respectively.

optimization. The calibrated method also achieves this minimum using about 50% less number of steps.

6 DISCUSSION AND RELATED WORK

Bayesian Optimization. Bayesian optimization is commonly used for optimizing black-box objective functions in applications like robotics [Calandra et al., 2016], reinforcement learning [Brochu et al., 2010], hyperparameter optimization [Bergstra et al., 2011], recommender systems [Vanchinathan et al., 2014], automatic machine learning, [Thornton et al., 2013] and materials design [Frazier and Wang, 2015]. The choices like acquisition function [Snoek et al., 2012], kernel function [Duvenaud et al., 2013] and transformation of input spaces [Snoek et al., 2014] are important in making sure that the optimization works efficiently.

Calibrated Uncertainties Platt scaling [Platt, 1999] and isotonic regression [Niculescu-Mizil and Caruana, 2005] are popular ways for calibrating uncertainties. This concept can be extended to regression calibration [Kuleshov et al., 2018], distribution calibration [Song et al., 2019], online learning [Kuleshov and Ermon, 2017b], and structured prediction [Kuleshov and Liang, 2015]. Accurate uncertainty representation has been studied for applications like model-based reinforcement learning [Malik et al., 2019], semi-supervised learning [Kuleshov and Ermon, 2017a], neural networks [Guo et al., 2017] and natural language processing models [Nguyen and O’Connor, 2015].

Limitations There are still some tasks such as SVHN image classification where calibration does not improve performance. Studying the properties of objective functions where calibrated Bayesian optimization produces lower benefits can be useful in identifying directions for further improvements in the algorithm.

Extensions & New Applications Bayesian optimization can use various underlying base models including neural networks [Snoek et al., 2015], which we have not yet explored. We would also like to apply our method to novel applications like Bayesian optimization for discovering chemical structures [Gómez-Bombarelli et al., 2018]. The recalibration dataset is small due to which the design of the calibration algorithm is important.

7 CONCLUSION

Bayesian optimization is used for optimizing black-box functions with minimal number of steps. Accuracy of uncertainty envelopes is important for balancing exploration-exploitation decisions which guide the iterative optimization process. We show that we can calibrate the underlying probabilistic model without using additional function evaluations. Our approach improves the average performance of Bayesian optimization in standard benchmark functions and hyperparameter optimization tasks.

References

The GPyOpt authors. Gpyopt: A bayesian optimization framework in python. <http://github.com/SheffieldML/GPyOpt>, 2016.

James Bergstra, Rémi Bardenet, Yoshua Bengio, and Balázs Kégl. Algorithms for hyper-parameter optimization. In J. Shawe-Taylor, R. Zemel, P. Bartlett, F. Pereira, and K. Q. Weinberger, editors, *Advances in Neural Information Processing Systems*, volume 24. Curran Associates, Inc., 2011. URL <https://proceedings.neurips.cc/paper/2011/file/86e8f7ab32cf12577bc2619bc635690-Paper.pdf>.

Eric Brochu, Vlad M. Cora, and Nando de Freitas. A tutorial on bayesian optimization of expensive cost functions, with application to active user modeling and hierarchical reinforcement learning, 2010.

R. Calandra, A. Seyfarth, and J Peters. Bayesian optimization for learning gaits under uncertainty. *Ann Math Artif Intell*, (76):5–23, 2016. URL <https://doi.org/10.1007/s10472-015-9463-9>.

David Duvenaud, James Robert Lloyd, Roger Grosse, Joshua B. Tenenbaum, and Zoubin Ghahramani. Structure discovery in nonparametric regression through compositional kernel search, 2013.

Peter I. Frazier. A tutorial on bayesian optimization, 2018.

Peter I. Frazier and Jialei Wang. Bayesian optimization for materials design. *Springer Series in Materials Science*, page 45–75, Dec 2015. ISSN 2196-2812. doi: 10.1007/978-3-319-23871-5_3. URL http://dx.doi.org/10.1007/978-3-319-23871-5_3.

Tilmann Gneiting and Adrian E Raftery. Strictly proper scoring rules, prediction, and estimation. *Journal of the American Statistical Association*, 102(477):359–378, 2007. doi: 10.1198/016214506000001437. URL <https://doi.org/10.1198/016214506000001437>.

Chuan Guo, Geoff Pleiss, Yu Sun, and Kilian Q. Weinberger. On calibration of modern neural networks, 2017.

Rafael Gómez-Bombarelli, Jennifer N. Wei, David Duvenaud, José Miguel Hernández-Lobato, Benjamín Sánchez-Lengeling, Dennis Sheberla, Jorge Aguilera-Iparraguirre, Timothy D. Hirzel, Ryan P. Adams, and Alán Aspuru-Guzik. Automatic chemical design using a data-driven continuous representation of molecules. *ACS Central Science*, 4(2):268–276, Jan 2018. ISSN 2374-7951. doi: 10.1021/acscentsci.7b00572. URL <http://dx.doi.org/10.1021/acscentsci.7b00572>.

Matthew Hoffman, Francis Bach, and David Blei. Online learning for latent dirichlet allocation. In J. Lafferty, C. Williams, J. Shawe-Taylor, R. Zemel, and A. Culotta, editors, *Advances in Neural Information Processing Systems*, volume 23. Curran Associates, Inc., 2010. URL <https://proceedings.neurips.cc/paper/2010/file/71f6278d140af599e06ad9bf1ba03cb0-Paper.pdf>.

Alex Krizhevsky. Learning multiple layers of features from tiny images. Technical report, 2009.

Volodymyr Kuleshov and Stefano Ermon. Deep hybrid models: bridging discriminative and generative approaches. In *Uncertainty in Artificial Intelligence*, 2017a.

Volodymyr Kuleshov and Stefano Ermon. Estimating uncertainty online against an adversary. In *AAAI*, pages 2110–2116, 2017b.

Volodymyr Kuleshov and Percy S Liang. Calibrated structured prediction. In C. Cortes, N. Lawrence, D. Lee, M. Sugiyama, and R. Garnett, editors, *Advances in Neural Information Processing Systems*, volume 28. Curran Associates, Inc., 2015. URL <https://proceedings.neurips.cc/paper/2015/file/52d2752b150f9c35ccb6869cbf074e48-Paper.pdf>.

Volodymyr Kuleshov, Nathan Fenner, and Stefano Ermon. Accurate uncertainties for deep learning using calibrated regression, 2018.

Balaji Lakshminarayanan, Alexander Pritzel, and Charles Blundell. Simple and scalable predictive uncertainty estimation using deep ensembles, 2016. URL <https://arxiv.org/abs/1612.01474>.

Ali Malik, Volodymyr Kuleshov, Jiaming Song, Danny Nemer, Harlan Seymour, and Stefano Ermon. Calibrated model-based deep reinforcement learning, 2019.

Yuval Netzer, Tao Wang, Adam Coates, Alessandro Bissacco, Bo Wu, and Andrew Y. Ng. Reading digits in natural images with unsupervised feature learning. In *NIPS Workshop on Deep Learning and Unsupervised Feature Learning 2011*, 2011. URL http://ufldl.stanford.edu/housenumbers/nips2011_housenumbers.pdf.

Khanh Nguyen and Brendan O’Connor. Posterior calibration and exploratory analysis for natural language processing models, 2015.

Alexandru Niculescu-Mizil and Rich Caruana. Predicting good probabilities with supervised learning. In *Proceedings of the 22nd International Conference on Machine Learning*, ICML ’05, page 625–632, New York, NY, USA, 2005. Association for Computing Machinery. ISBN 1595931805. doi: 10.1145/1102351.1102430. URL <https://doi.org/10.1145/1102351.1102430>.

John C. Platt. Probabilistic outputs for support vector machines and comparisons to regularized likelihood methods. In *ADVANCES IN LARGE MARGIN CLASSIFIERS*, pages 61–74. MIT Press, 1999.

Gonzalo Rios and Felipe Tobar. Learning non-gaussian time series using the box-cox gaussian process. pages 1–8, 07 2018. doi: 10.1109/IJCNN.2018.8489648.

Glenn Shafer and Vladimir Vovk. A tutorial on conformal prediction. 2007. doi: 10.48550/ARXIV.0706.3188. URL <https://arxiv.org/abs/0706.3188>.

Babak Shahriari, Kevin Swersky, Ziyu Wang, Ryan P. Adams, and Nando de Freitas. Taking the human out of the loop: A review of bayesian optimization. *Proceedings of the IEEE*, 104(1):148–175, 2016. doi: 10.1109/JPROC.2015.2494218.

Edward Snelson, Zoubin Ghahramani, and Carl Rasmussen. Warped gaussian processes. In S. Thrun, L. Saul, and B. Schölkopf, editors, *Advances in Neural Information Processing Systems*, volume 16. MIT Press, 2004. URL <https://proceedings.neurips.cc/paper/2003/file/6b5754d737784b51ec5075c0dc437bf0-Paper.pdf>.

Jasper Snoek, Hugo Larochelle, and Ryan P. Adams. Practical bayesian optimization of machine learning algorithms. In *Proceedings of the 25th International Conference on Neural Information Processing Systems - Volume 2*, NIPS’12, page 2951–2959, Red Hook, NY, USA, 2012. Curran Associates Inc.

Jasper Snoek, Kevin Swersky, Richard S. Zemel, and Ryan P. Adams. Input warping for bayesian optimization of non-stationary functions, 2014.

Jasper Snoek, Oren Rippel, Kevin Swersky, Ryan Kiros, Nadathur Satish, Narayanan Sundaram, Mostofa Patwary, Mr Prabhat, and Ryan Adams. Scalable bayesian optimization using deep neural networks. In Francis Bach and David Blei, editors, *Proceedings of the 32nd International Conference on Machine Learning*, volume 37 of *Proceedings of Machine Learning Research*, pages 2171–2180, Lille, France, 07–09 Jul 2015. PMLR. URL <http://proceedings.mlr.press/v37/snoek15.html>.

Hao Song, Tom Diethe, Meelis Kull, and Peter Flach. Distribution calibration for regression, 2019.

Jost Tobias Springenberg, Aaron Klein, Stefan Falkner, and Frank Hutter. Bayesian optimization with robust bayesian neural networks. In D. Lee, M. Sugiyama, U. Luxburg, I. Guyon, and R. Garnett, editors, *Advances in Neural Information Processing Systems*, volume 29. Curran Associates, Inc., 2016. URL <https://proceedings.neurips.cc/paper/2016/file/a96d3afec184766bfeca7a9f989fc7e7-Paper.pdf>.

S. Surjanovic and D. Bingham. Virtual library of simulation experiments: Test functions and datasets. Retrieved October 8, 2022, from <http://www.sfu.ca/~ssurjano>.

Chris Thornton, Frank Hutter, Holger H. Hoos, and Kevin Leyton-Brown. Auto-weka: Combined selection and hyperparameter optimization of classification algorithms, 2013.

Hastagiri P. Vanchinathan, I. Nikolic, F. D. Bona, and Andreas Krause. Explore-exploit in top-n recommender systems via gaussian processes. In *RecSys ’14*, 2014.

Vladimir Vovk, Ivan Petej, Paolo Tocacceli, Alexander Gammerman, Ernst Ahlberg, and Lars Carlsson. Conformal calibrators. In Alexander Gammerman, Vladimir Vovk, Zhiyuan Luo, Evgeni N. Smirnov, Giovanni Cherubin, and Marco Christini, editors, *Conformal and Probabilistic Prediction and Applications, COPA 2020, 9–11 September 2020, Virtual Event, Verona, Italy*, volume 128 of *Proceedings of Machine Learning Research*, pages 84–99. PMLR, 2020. URL <http://proceedings.mlr.press/v128/vovk20a.html>.

Shengjia Zhao, Tengyu Ma, and Stefano Ermon. Individual calibration with randomized forecasting, 2020. URL <https://arxiv.org/abs/2006.10288>.

A ADDITIONAL DETAILS ON EXPERIMENTS

We implement our method on top of the GPyOpt library [authors, 2016] (BSD 3 Clause License) in Python. The output values of objective function are normalized before training the base GP model. The GP uses Radial Basis Function (RBF) kernel. For the experiments on hyperparameter optimization tasks, we used Expected Improvement as acquisition function. We use 5 randomly chosen data-points to initialize the base GP. The experiments are repeated 5 times and the results are averaged over these 5 runs.

Table 4: Comparison of Calibrated Bayesian Optimization Against Baselines. We see that the calibrated method compares favorably against Input warping ([Snoek et al., 2014]), Output warping (tanh as in [Snelson et al., 2004]), Boxcox and Log transformation of output ([Rios and Tobar, 2018]), and Bagged ensemble of 5 GPs ([Lakshminarayanan et al., 2016]).

Objective Function	Method	Minimum Found (↓)	Fraction of Runs Where Calibrated Beats Baseline (↑)	Area Under the Curve (↓)
Forrester (1D)	Calibrated Method	-4.983 (0.894)	1	0.8187
	Uncalibrated method	-0.986 (0.001)	0.8	0.9866
	Input warping	-0.889 (0.000)	1	1.0000
	Output warping	-6.021 (0.000)	0.0	0.2409
	Boxcox transformation of output	-4.806 (0.780)	0.4	0.4911
	Log transformation of output	-0.986 (0.000)	1	0.9865
	Bagged ensemble of 5 GPs	-3.891 (1.098)	0.8	0.8382
Ackley (2D)	Calibrated Method	5.998 (2.314)	1	0.5516
	Uncalibrated method	12.359 (2.439)	0.8	0.7815
	Input warping	14.061 (1.312)	0.8	0.8125
	Output warping	10.459 (3.365)	0.6	0.7257
	Boxcox transformation of output	14.421 (1.423)	0.8	0.9015
	Log transformation of output	8.330 (0.849)	0.8	0.6524
	Bagged ensemble of 5 GPs	6.011 (2.544)	0.6	0.6013
Cosines (2D)	Calibrated Method	-1.5983 (0.0006)	1	0.2969
	Uncalibrated method	-1.5974 (0.00102)	0.8	0.3441
	Input warping	-1.3054 (0.0347)	1.0	0.9534
	Output warping	-1.5994 (0.0001)	0.8	0.4730
	Boxcox transformation of output	-1.5306 (0.0590)	0.8	0.5969
	Log transformation of output	-1.5992 (0.0003)	0.8	0.3642
	Bagged ensemble of 5 GPs	-1.5989 (0.0003)	0.4	0.3179
Alpine (10D)	Calibrated Method	12.537 (0.909)	1	0.6423
	Uncalibrated method	15.506 (1.275)	0.6	0.6527
	Input warping	15.697 (1.740)	0.8	0.6492
	Output warping	13.531 (2.127)	0.6	0.5857
	Boxcox transformation of output	15.715 (0.603)	0.8	0.6253
	Log transformation of output	20.996 (1.661)	0.8	0.7931
	Bagged ensemble of 5 GPs	16.677 (1.699)	0.8	0.7334

A.1 Evaluation Metrics

We define the following metrics to compare calibrated Bayesian optimization with uncalibrated method and other baselines.

1. Minimum value m of the objective function achieved by Bayesian optimization. Lower values of m are better.
2. Fraction f of experimental repetitions where the baseline performs worse than our method. A baseline performs worse than our method if it does not find a lower minimum, if it finds the

same minimum in a larger number of steps, or if its optimization curve is entirely above that of the calibrated method. Higher values of f are better.

3. Normalized area under the optimization curve a . For each method, we compute the area under its optimization curve (i.e., its optimum as a function of the number of optimization steps; see Figure 2) and normalize it relative to the area of the rectangle formed by upper and lower bounds along the x , y axes (hence $\max a$ is one). Smaller values of a indicate that the method reaches the minimum faster, hence are better.

A.2 Comparison of Calibrated Bayesian Optimization Against Other Baselines

We produce additional results on this comparison in Table 4.

A.3 Sensitivity Analysis

We produce additional results on sensitivity analysis in Table 5.

Table 5: Sensitivity Analysis of Calibrated Bayesian Optimization Algorithm for the Forrester Function.

Hyper-Parameter	Modification	% Runs Where Calibrated is Best (\uparrow)	Area Under the Curve, Calibrated (\downarrow)	Area Under the Curve, Uncalibrated (\downarrow)
Kernel of Base Model \mathcal{M}	Matern	0.8	0.2811	0.3454
	Linear	1.0	0.5221	1.0000
	RBF	0.4	0.2366	0.2922
	Periodic	0.6	0.2586	0.3305
Number of Time-series splits in CREATESPLITS	N-1	0.8	0.2811	0.3454
	N-2	0.8	0.2768	0.3454
	N-3	0.8	0.2653	0.3454
	N-4	0.6	0.2643	0.3454
Recalibrator Model \mathcal{R}	GP	0.8	0.2810	0.3454
	MLP	0.8	0.2785	0.3454
Number of Data Points for Initializing Base Model	3	0.8	0.2810	0.3454
	4	0.8	0.0557	0.0614
	7	0.4	0.0719	0.0736
	10	0.4	0.0825	0.0817
Initialization Design (Base model initialized with 4 data points)	Random	0.8	0.0557	0.0614
	Sobol	0.6	0.0415	0.0414
	Latin	0.2	0.2358	0.2181
Acquisition function (Linear kernel)	LCB	1.0	1.0000	1.0000
	EI	1.0	0.5221	1.0000
	PI	0.8	0.6920	1.0000

A.4 Online LDA

We use the grid of parameters mentioned in Table 6 as the input domain while running Bayesian optimization. We run this algorithm on the 20 Newsgroups dataset which contains 20,000 news documents partitioned evenly across 20 different newsgroups. We train the algorithm on 11,000 randomly chosen documents. A test-dataset of 2200 articles is used to assess the perplexity.

Table 6: Hyperparameters for Online LDA

Name of HP	Bounds	Type of domain
Minibatch size	[1, 128]	Discrete (log-scale)
κ	[0.5, 1]	Continuous (step-size=0.1)
τ_0	[1, 32]	Discrete (log-scale)

A.5 Image Classification Using Neural Networks

We provide the range of hyperparameters considered while performing Bayesian optimization to determine their optimal configuration with reference to the image classification experiments in Table 7.

Table 7: Hyperparameters for CNN (CIFAR10 and SVHN classification)

Name of HP	Bounds	Type of domain
Batch size	[32, 512]	Discrete (step size 32)
Learning rate	[0.0000001, 0.1]	Continuous (log-scale)
Learning rate decay	[0.0000001, 0.001]	Continuous (log-scale)
L2 regularization	[0.0000001, 0.001]	Continuous (log-scale)
Outchannels in fc layer	[256, 512]	Discrete (step size=16)
Outchannels in conv layer	[128, 256]	Discrete (step size=16)

B CALIBRATION OF PROBABILISTIC MODEL

For training a recalibrator over our probabilistic model, we compute the CDF F_t at each data-point y_t using the formulation $F_t = [\mathcal{M}(x_t)](y_t)$. This can be used to estimate the empirical fraction of data-points below each quantile. Algorithm 4 based on Kuleshov et al. [2018] outlines this procedure.

Algorithm 4: Calibration of Probabilistic Model

Input: Dataset of probabilistic forecasts and outcomes $\{[\mathcal{M}(x_t)](y_t), y_t\}_{t=1}^N$

1. Form recalibration set $\mathcal{D} = \{[F_t, \hat{P}(F_t)]\}_{t=1}^N$ where $F_t = [\mathcal{M}(x_t)](y_t)$ and $\hat{P}(p) = |\{y_t \mid [F_t \leq p, t = 1, \dots, N]\}|/N$.
2. Train recalibrator model \mathcal{R} on dataset \mathcal{D} .

C EXAMINING AQUISITION FUNCTIONS

We analyze the role of calibration in common acquisition functions used in Bayesian optimization.

Probability of Improvement. The probability of improvement is given by $P(f(x) \geq (f(x^+) + \epsilon))$, where $\epsilon > 0$ and x^+ is the previous best point. Note that this corresponds to $1 - F_x(f(x^+) + \epsilon)$, where F_x is the CDF at x that is predicted by the model. In a quantile-calibrated model, these probabilities on average correspond to the empirical probability of observing an improvement event. This leads to acquisition function values that more accurately reflect the value of exploring specific regions. Furthermore, if the model is calibrated, we keep working with calibrated values throughout the optimization process, as x^+ changes.

Expected Improvement. The expected improvement can be defined as $\mathbb{E}[\max(f(x) - f(x^+), 0)]$. This corresponds to computing the expected value of the random variable $R = \max(Y - c, 0)$, where Y is the random variable that we are trying to model by \mathcal{M} , and $c \in \mathbb{R}$ is a constant. If we have a calibrated distribution over Y , it is easy to derive from it a calibrated distribution over R . By Proposition 2, we can estimate $\mathbb{E}[R]$ under the calibrated model, just as we can estimate the probability of improvement in expectation.

Upper Confidence Bounds. The UCB acquisition function for a Gaussian process is defined as $\mu(x) + \gamma \cdot \sigma(x)$ at point x . For non-Gaussian models, this naturally generalizes to a quantile $F_x^{-1}(\alpha)$ of the predicted distribution F . In this context, recalibration adjusts confidence intervals such that $\alpha \in [0, 1]$ corresponds to an interval that is above the true y a fraction α of the time. This makes it easier to select a hyper-parameter α . Moreover, as α or γ are typically annealed, calibration induces a better and smoother annealing schedule.

D ADDITIONAL DISCUSSION

A key conceptual contribution of our work is a new angle for reasoning about uncertainty in the context of sequential decision-making. There exist many known decompositions of uncertainty, e.g. epistemic vs. aleatoric. Our work argues for using a different decomposition of uncertainty that is rarely used: calibration + sharpness.

This decomposition is interesting because the calibration property can be easily enforced in practice; at the same time this property greatly improves sequential decision-making for reasons we explain in the paper, and enforcing it results in significant practical benefits. This fact is currently underappreciated; our work contributes to a body of literature (see e.g., Malik et al. [2019]) that helps popularize the idea of reasoning about uncertainty through the lens of calibration and sharpness, and can lead to significant practical improvements in uncertainty-aware algorithms that adopt our angle.

From a methodological perspective, our work resolves challenges in applying calibration in the context of Bayesian optimization. We introduce recalibration mechanisms based on leave-one-out cross-validation with a temporal ordering and we design specific classes of Gaussian recalibrators that are compatible with GP outputs and acquisition function inputs. We discovered that more naive applications of calibration fail, and our methods are non-trivial. Finally, we show empirically that our ideas have significant practical benefits.

D.1 On the Computational Cost of Calibrated Bayesian Optimization

Calibration increases the computational cost of Bayesian optimization (since we fit multiple GP models, and not just one). However, in most applications, we expect that the cost of fitting GPs will be negligible compared to the cost of evaluating the objective function at a datapoint. For example, in hyper-parameter optimization, the cost of training a new neural network with a new

set of hyper-parameters vastly exceeds the cost of fitting a GP. Hence, calibrated and uncalibrated methods are in practice comparable in terms of their computational costs, and training multiple GPs does not limit the applicability of our method.

D.2 On Epistemic vs. Aleatoric Uncertainties

Our method calibrates both epistemic and aleatoric uncertainties equally well. The concept of calibration is complementary and orthogonal to the concept of epistemic vs. aleatoric uncertainty. Our method takes any probabilistic prediction $P(y)$ over y (regardless of whether uncertainties $P(y)$ are epistemic or aleatoric) and recalibrates it, resulting in improved performance.

Specifically, let $\mathcal{M}(x)$ be a probabilistic model that outputs a probabilistic forecast $P(y)$ over the target y . The $\mathcal{M}(x)$ may model purely aleatoric uncertainties (e.g., \mathcal{M} is a neural network with a softmax or Gaussian output layer) or epistemic uncertainties (e.g., \mathcal{M} is a GP). In either case, $P(y)$ is just a distribution for which we can assess calibration. Our method improves calibration equally well regardless of the type of $\mathcal{M}(x)$ that generated $P(y)$. Improved calibration in turn increases optimization performance of both Bayesian and non-Bayesian base models $\mathcal{M}(x)$. For more details, please consider the analysis of Bayesian and non-Bayesian methods by Kuleshov et al. [2018] (our work extends their recalibration technique and inherits its properties).

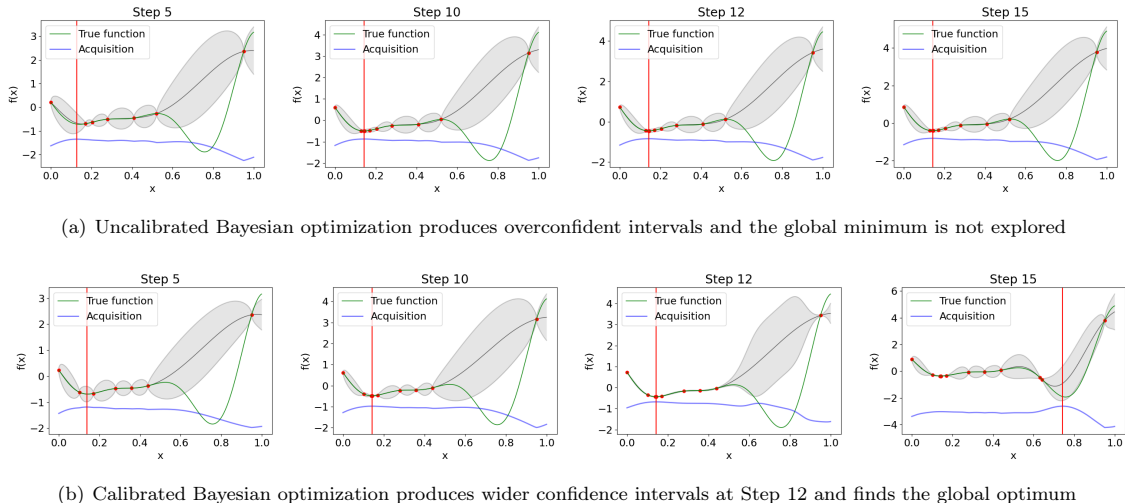


Figure 5: Selected steps of uncalibrated and calibrated Bayesian optimization on the Forrester function (green) using the UCB acquisition function (blue). The global minimum lies near 0.8; however, after sampling 3 initial points at random, the model is constant in $[0.6, 0.9]$, while the true function has a large dip. Since confidence intervals in $[0.6, 0.9]$ are fairly narrow in the uncalibrated method, and the optimization algorithm never explores it, the global minimum is missed by a large margin. In the calibrated method however, the recalibrator learns after iteration 12 that the model is overconfident, expanding its confidence intervals. This leads the calibrated model to explore in $[0.6, 0.9]$ and find the global minimum.

D.3 On Sensitivity With Respect to the Gaussian Assumption

The effects of the Gaussian assumption can be seen in Table 3. These additional tasks cover benchmark functions which are closer (e.g. cosines) and farther (e.g. cross-in-tray) from Gaussian assumptions. We do observe lower performance of both calibrated and uncalibrated Bayesian optimization methods on non-Gaussian tasks. This suggests an opportunity to improve Bayesian optimization by leveraging non-Gaussian models as a replacement for the classical GP approach.

D.4 On Sensitivity With Respect to Higher Dimensions

In the paper, we have results for the Alpine function in 10 dimensions and the hyperparameter optimization tasks have 3-6 input dimensions each. Thus, we observe the benefits of calibration in higher dimensions as well. However, we did observe that in higher dimensions the improvement offered by calibration starts to become gradually less pronounced, which may be attributed to the curse of dimensionality (the difficulty of estimating densities in high dimensions).

E ANALYSING CALIBRATION FOR FORRESTER FUNCTION

In Figure 5, we see a visual comparison of optimization performed by calibrated method against the uncalibrated method.

F MATHEMATICAL PROOFS

F.1 Notation and Preliminaries

We assume there exists a data distribution P over features and labels $X, Y \in \mathcal{X} \times \mathbb{R}$, and we are given an initial labeled dataset $x_t, y_t \in \mathcal{X} \times \mathbb{R}$ for $t = 1, 2, \dots, N$ of i.i.d. realizations of random variables $X, Y \sim P$. Bayesian optimization is a technique for finding the global minimum $x^* = \arg \min_{x \in \mathcal{X}} f(x)$ of an unknown black-box objective function $f : \mathcal{X} \rightarrow \mathbb{R}$ over an input space $\mathcal{X} \subseteq \mathbb{R}^D$. Crucially, Bayesian optimization relies on a probabilistic model H that given X outputs a predictive distribution over Y ; it uses this model to select the next point as part of a larger optimization procedure.

Formally, suppose we have a model $H : \mathcal{X} \rightarrow (\mathbb{R} \rightarrow [0, 1])$ that outputs a probabilistic forecast F_x given an input x . We take F_x to be a cumulative distribution function (CDF) and we use $F_X^{-1}(p) = \inf\{y : F_X(y) = p\}$ to denote its inverse, the quantile function. We will use f_X to denote the associated density function.

F.1.1 Distribution Calibration

We say that H outputs distribution calibrated forecasts if the true density of Y conditioned on the forecaster predicting a density of f also equals f :

$$P(Y | H(X) = f) = f \quad \forall f.$$

For example, if the model H outputs Gaussian predictive distributions over Y with parameters $\mu(X), \sigma(X)$, we are asking that conditioned on the prediction $\mu(X), \sigma(X)$, the true distribution of Y is also a Gaussian with parameters $\mu(X), \sigma(X)$.

In practice, the model $H(X)$ produces predictive distributions by outputting a set of parameters $\phi(X)$ in a set Φ that induces a density $f(Y; \phi)$. Thus, we use the following definition of distribution calibration:

$$P(Y | H(X) = \phi) = f(Y; \phi) \quad \forall \phi \in \Phi.$$

F.1.2 Quantile Calibration

We say that H outputs quantile calibrated forecasts if $P(Y \leq F_X^{-1}(p)) = p \quad \forall p \in [0, 1]$. Here, $F_X^{-1}(p)$ is the inverse for CDF value p . It is defined as $F_X^{-1}(p) = \inf\{y : F_X(y) = p\}$ where $F_X(y)$ outputs the CDF over output y for given input x to the model H . In an online setting this definition becomes

$$\frac{\sum_{t=1}^T \mathbb{I}\{y_t \leq F_t^{-1}(p)\}}{T} \rightarrow p \text{ for all } p \in [0, 1] \quad (8)$$

as $T \rightarrow \infty$, hence the predicted and empirical confidence intervals match. Equivalent formulations used in this paper include

$$P(Y \leq y | F_X(Y) = p) = p, \quad \forall p \in [0, 1].$$

We define calibration in Bayesian optimization analogously to Kuleshov et al. [2018] and Malik et al. [2019]. We say that a Bayesian optimization model $\mathcal{M} : \mathcal{X} \rightarrow (\mathbb{R} \rightarrow [0, 1])$ is calibrated if $P(Y \leq F_X^{-1}(p)) = p \quad \forall p \in [0, 1]$, where $F_X : \mathbb{R} \rightarrow [0, 1]$ is the CDF forecast $\mathcal{M}(X)$.

F.1.3 Loss functions and Bayesian Decision-Making

In decision-making settings such as Bayesian optimization, we are working with loss functions $\ell : \mathcal{Y} \times \mathcal{A} \rightarrow \mathbb{R}$, where \mathcal{Y} is the space of outcomes ($\mathcal{Y} = \mathbb{R}$ in this paper) and \mathcal{A} is the set of possible actions the decision-making agent can take. The loss function $\ell(y, a')$ quantifies the error of performing an action $a \in \mathcal{A}$ when the realized outcome is $y \in \mathcal{Y}$.

Bayesian decision-making theory provides a principled approach for selecting actions in the above scenario. We rely on a predictive model H of y and select decisions that minimize the expected loss:

$$a(x) = \arg \min_a \mathbb{E}_{y \sim H(x)}[\ell(y, a)] \quad (9)$$

$$\ell(x) = \min_a \mathbb{E}_{y \sim H(x)}[\ell(y, a)]. \quad (10)$$

Here, $a(x)$ and $\ell(x)$ denote, respectively, the action that minimizes the expected loss under H given auxiliary features x and $\ell(x)$ is the corresponding value of the estimated expected loss.

If H was a perfect predictive model, the above decision-making approach would be optimal. In practice, inaccurate models can yield imperfect decisions. Surprisingly, our analysis shows that in many cases, calibration (a much weaker condition than having a perfectly specified model H) is sufficient to correctly estimate the value of the loss function.

Monotonic Loss Functions Specifically, we restrict our attention to a number of common loss functions. A monotonic loss function $\ell(y, a)$ is either monotonically non-increasing or non-decreasing in a . Examples of monotonic losses include linear utilities such as $v(a) \cdot y + c(a)$ or their monotonic transformations (e.g., $v(a) \cdot \log y + c(a)$). Note that common acquisition functions used in Bayesian optimization fall in this framework.

F.2 Distribution Calibrated Models

The strongest form of calibration is distribution calibration, and is what we normally think of calibration in the context of applications such as weather forecasting. Distribution calibration has the property of being able to provide accurate estimates of expectations even when the predictive model is mis-specified (but is still distribution calibrated). This fact was originally established by Malik et al. (2019) in the discrete settings; here, we extend this result to general distributions over continuous variables.

Proposition 1. *Let $Q(Y|X)$ be a distribution calibrated model over $X, Y \sim P$ such that $P(Y = y | Q(Y = y | X) = \phi) = \phi$, where $\phi \in \Phi$ represents parameters of the probability distribution. Then, for any function $g : \mathbb{Y} \rightarrow \mathcal{S}$ with which we want to take an expectation, the following equality holds:*

$$\mathbb{E}_{y \sim P(Y)} [g(y)] = \mathbb{E}_{\substack{x \sim P(X) \\ y \sim Q(Y|X=x)}} [g(y)]. \quad (11)$$

Proof. First, observe that we can write:

$$\begin{aligned} \mathbb{E}_{y \sim P(Y)} [g(y)] &= \int g(y) P(Y = y) dy \\ &= \int g(y) \int_{\phi \in \Phi} P(Y = y, Q(Y = y | X) = \phi) d\phi dy \\ &= \int g(y) \int_{\phi \in \Phi} P(Y = y | Q(Y = y | X) = \phi) P(Q(Y = y | X) = \phi) d\phi dy. \end{aligned}$$

In the second line, we used the law of total probability and in the third line, we used the chain rule of probability. We use the notation $\{Q(Y = y | X) = p\}$ to refer to the event $\{X | Q(Y = y | X) = p\}$.

Next, we use our calibration assumption $P(Y = y | Q(Y = y | X) = p) = p$ and prove our claim as follows:

$$\begin{aligned} \mathbb{E}_{y \sim P(Y)} [g(y)] &= \int g(y) \int_{\phi \in \Phi} \phi \cdot P(Q(Y = y | X) = \phi) d\phi dy \\ &= \int g(y) \int_{\phi \in \Phi} \phi \cdot \int_{Q(Y = y | X = x) = \phi} P(X = x) dx d\phi dy \\ &= \int g(y) \int Q(Y = y | X = x) \cdot P(X = x) dx dy \\ &= \int P(X = x) \sum g(y) \cdot Q(Y = y | X = x) dy dx \\ &= \mathbb{E}_{x \sim P(X)} \mathbb{E}_{y \sim Q(Y|X=x)} [g(y)]. \end{aligned}$$

□

The requirement of distribution calibration is weaker than the requirement of a well-specified predictive model. However, it is still challenging to enforce. Below, we show that this requirement can be replaced by a much weaker notion of quantile calibration.

F.3 Quantile Calibrated Models

Surprisingly, the guarantees for distribution calibrated models can be obtained with a much weaker notion of calibration—quantile calibration.

F.3.1 Accurate Estimation of Expectations

Similarly to the previous result, we can accurately compute expectations using a model that is simply quantile calibrated (rather than distribution calibrated). The key additional requirement is non-negativity on the random variable whose expectation is being computed.

Proposition 2. *Let Y be a non-negative random variable. Let $Q(Y|X)$ be a quantile calibrated model over $X, Y \sim P$ such that $P(Y \geq y | Q(Y \geq y | X) = p) = p$. Then the expectation of Y is the same under P and Q :*

$$\mathbb{E}_{y \sim P(Y)} [y] = \mathbb{E}_{x \sim P(X)} \mathbb{E}_{y \sim Q(Y|X=x)} [y]. \quad (12)$$

Proof. In this proof, we will use the well-known identity that for a non-negative Y ,

$$\mathbb{E}[Y] = \int_0^\infty F(Y \geq y) dy,$$

where F is the CDF of Y .

Next, note that we can rewrite the expectation on the LHS of Equation 12 as:

$$\begin{aligned} \mathbb{E}_{y \sim P(Y)} [y] &= \int_0^\infty P(Y \geq y) dy \\ &= \int_0^\infty \int_0^1 P(Y \geq y | Q(Y \geq y | X) = p) dp dy \\ &= \int_0^\infty \int_0^1 \left(P(Y \geq y | Q(Y \geq y | X) = p) \right. \\ &\quad \left. P(Q(Y \geq y | X) = p) \right) dp dy \end{aligned}$$

where we used the above identity in the first line, the law of total probability in the second line, and the chain rule in the third line.

Next, we can use our assumption on the calibration of Q to replace one of the terms with p , further expanding the above into:

$$\begin{aligned} \mathbb{E}_{y \sim P(Y)} [y] &= \int_0^\infty \int_0^1 p \cdot P(Q(Y \geq y | X) = p) dp \\ &= \int_0^\infty \int_0^1 p \cdot \int_{x \in \mathbb{X}} \mathbb{I}[Q(Y \geq y | X = x) = p] \cdot P(X = x) dx dp \\ &= \int_0^\infty \int_{x \in \mathbb{X}} Q(Y \geq y | X = x) \cdot P(X = x) dx \\ &= \int_{x \in \mathbb{X}} P(X = x) \int_0^\infty Q(Y \geq y | X = x) dx \\ &= \mathbb{E}_{x \sim P(X)} \mathbb{E}_{y \sim Q(Y|X=x)} [y], \end{aligned}$$

where in the last line we again used the identity $\mathbb{E}[Y] = \int_0^\infty F(Y \geq y) dy$. This completes the proof. \square

We can use the above result to establish an analogue of the guarantee available for distribution calibration

Proposition 3. *Let $Q(Y|X)$ be a quantile calibrated model over $X, Y \sim P$. Then, for any non-negative monotonic function $g : \mathbb{Y} \rightarrow \mathcal{S}$ with which we want to take an expectation, the following equality holds:*

$$\mathbb{E}_{y \sim P(Y)} [g(y)] = \mathbb{E}_{\substack{x \sim P(X) \\ y \sim Q(Y|X=x)}} [g(y)]. \quad (13)$$

Proof. This result follows from the previous lemma. Since Q is a quantile-calibrated model for Y , we also have that $g \circ Q$ is a quantile calibrated model for the random variable $g(Y)$ when g is monotonically increasing:

$$P(g(Y) \leq g(Q_X(p))) = p.$$

A similar argument applies when g is monotonically decreasing. In both cases, we have that $g(Q_X(p))$ is a calibrated quantile function for $g(Y)$ and hence our claim follows directly from the previous result. \square

F.3.2 Divergence Bounds

We have shown that a calibrated model can be used to estimate expectations on average. Here, we complement these results with additional concentration inequalities that show that estimated of the calibrated loss are unlikely to exceed the true loss. Note that this statement represents an extension of Markov inequality.

Proposition 4. *Let $Q(Y|X)$ be a quantile calibrated model over $X, Y \sim P$. Let $\ell(y, a)$ be a monotonically non-decreasing or non-increasing loss and let $a(X) = \arg \min_a \mathbb{E}_{y \sim Q(y|x)}[\ell(y, a)]$ and $\ell(x) = \min_a \mathbb{E}_{y \sim Q(y|x)}[\ell(y, a)]$ be the optimal action under Q and its loss respectively. Then we have for $t > 1$:*

$$P(\ell(y, a(x)) \geq t\ell(x)) \leq 1/t \quad (14)$$

Proof. Let F_Q be the CDF associated with Q . Note that for any x and $s \in (0, 1)$ and $y' \leq F_Q^{-1}(1-s)$ we have:

$$\begin{aligned} \ell(x) &= \int \ell(x, y, a(x))Q(y|x)dy \\ &\geq \int_{y \geq y'} \ell(x, y, a(x))Q(y|x)dy \\ &\geq \ell(x, y', a(x)) \int_{y \geq y'} Q(y|x)dy \\ &\geq s\ell(x, y', a(x)) \end{aligned}$$

The above logic implies that whenever $\ell(x) \leq s\ell(x, y, a)$, we have $y \geq F_Q^{-1}(1-s)$ or $F_Q(y) \geq (1-s)$. Thus,

$$P(\ell(x) \leq s\ell(x, y, a)) \leq P(F_Q(y) \geq (1-s)) = s,$$

where the last equality follows because Q is calibrated. Therefore the claim holds with $t = 1/s$.

The argument is similar if ℓ is monotonically non-increasing. In that case, we can show that whenever $y' > F_Q^{-1}(s)$, we have $\ell(x) \geq s\ell(x, y', a(x))$. Thus, whenever $\ell(x) \leq s\ell(x, y, a)$, we have $y \leq F_Q^{-1}(s)$ or $F_Q(y) \leq s$. Because, F is calibrated, we again have that

$$P(\ell(x) \leq s\ell(x, y, a)) \leq P(F_Q(y) < s) = s,$$

and the claim holds with $t = 1/s$. \square

Using this result, we can also show that the same guarantees can be established for distribution calibration, since the latter implies quantile calibration.

Proposition 5. *Let $Q(Y|X)$ be a distribution calibrated model over $X, Y \sim P$. Let $\ell(y, a)$ be a monotonically non-decreasing or non-increasing loss and let $a(X) = \arg \min_a \mathbb{E}_{y \sim Q(y|x)}[\ell(y, a)]$ and $\ell(x) = \min_a \mathbb{E}_{y \sim Q(y|x)}[\ell(y, a)]$ be the optimal action under Q and its loss respectively. Then we have for $t > 1$:*

$$P(\ell(y, a(x)) \geq t\ell(x)) \leq 1/t \quad (15)$$

Proof. This follows directly from the fact that a distribution calibrated model is also quantile calibrated. \square